Investigation of a Potential Drug Delivery System Using Hollow Gold Nanoparticles

Hana Miller

Senior Comprehensive Project

September 14, 2023



Department of Biochemistry

Submitted to the Department of Biochemistry of Allegheny College in partial fulfillment of the requirement for the degree of Bachelor of Science.

Investigation of a Potential Drug Delivery System Using Hollow Gold Nanoparticles

Hana Miller

Senior Comprehensive Project

Allegheny College - Class of 2024

Committee Members:

Dr. Alice Deckert (Research Advisor)

Dr. Ivelitza Garcia

Dr. Margaret Nelson

I hereby recognize and pledge to fulfill my responsibilities as defined in the Honor Code, and to maintain the integrity of myself and the college community.

Pledge: _____

Investigation of a Potential Drug Delivery System Using Hollow Gold Nanoparticles

Table of Contents

ACKNOWLEDGEMENTS …… 3

ABSTRACT …… 5

INTRODUCTION …….. 6

Figure 1 ……. 7

Figure 2 ……. 11

Figure 3 ……. 14

Figure 4 ……. 15

MATERIALS AND METHODS ……..…… 22

RESULTS AND DISCUSSION …….. 25

SILVER NANOPARTICLE SYNTHESIS ……. 25

Figure 5 …….. 26

HOLLOW GOLD NANOPARTICLE SYNTHESIS ……...…… 26

Figure 6 ……. 27

LOADING STUDIES ……... 28

Figure 7 ……. 28

Figure 8 ……. 29

Figure 9 ……. 30

FUTURE DIRECTIONS …….. 34

CONCLUSION ……. 35

RESOURCES …… 36

Acknowledgements:

This project would not have been completed and successful without the support and encouragement of special people in my life. I would like to thank everyone that has helped, not only for this project, but for making my time here the best it could be. My class especially has faced hard times and events that no one could prepare us for. As a result, we have grown as individuals who now focus on the good in life and see hope in dark places.

I would first like to thank my Advisor, Dr. Deckert, who's worked incredibly hard to help make me successful. I am beyond appreciative of your encouragement, belief, help, and hard work you have put into this project and department. This project would not be what it is without your ideas and helpful criticism that pushed me throughout my time at Allegheny College. I would also like to thank my Academic Advisor, Dr. Garia who has guided me throughout my time here at Allegheny College and who's continuous support has helped me be successful. I also thank Dr. Nelson for your support, encouragement, and laughs throughout my years here at Allegheny College. These professors have all been a support system and backbone for me throughout this project whom I cannot thank enough for their contributions.

To my Lord and Savior, thank you always for everything. To Mom, Dad, and Sara, I thank you so much. For listening to my rants about my comp, for showing up when I needed you most, and for being a shoulder I can lean on when I am in tough spots. Your support and endless love are what got me through these four years and I do not know where I would be without you guys. Thank you mom and dad for allowing me to have the opportunity to go to school here and write about something that is so beyond cool, and for supporting me in my decision to continue my education at Regent University School of Law. I also would like to thank my parents for being my biggest cheerleaders. Both of you are always the first to share my news and successes

with the world. To Everest, my partner in crime, I know you cannot read but know you've helped me through a lot of dark times and I share my degree with you! Thank you for being my best friend and for always being there for me. To my friends, thank you for getting me out of my room when I holed up from working too hard, being my rock when things got too tough, and always making me laugh. I will only be a call away! Thank you to my field hockey team who has encouraged me throughout my career. To my sisters of Kappa Kappa Gamma, thank you for always being there for me. You guys have been there for me through it all and I am so grateful that I am a part of an institution that inspires, uplifts, and supports each other. To each of you, you will change the world one day and I am so proud of you all! L+L Mills!

Finally, I would like to thank Allegheny College. I have grown so much as a person throughout these four years. I have had a lot of ups and downs, but I am thankful for the friends, love, and knowledge this institution has brought me along the way. Now that I am at the end of this chapter, I know a new one is just beginning. I am confident that Allegheny College has prepared me for the future and I cannot wait to see what Law School has in store for me. CHEERS!

Abstract:

Sodium Borohydride was used to synthesize silver nanoparticles (AgNPs) for a galvanic replacement reaction to obtain hollow gold nanoparticles (HAuNPs). The HAuNPs have a resonance peak at 980 nm which have properties that are reliable for a potential drug delivery system and target therapy treatment for cancer. Methyl Orange, Chrysoine Resorcinol, and Acid Orange 5 dyes were used as a model for loading a drug into the HAuNPs. The dyes were used to determine if polarity and bulk have an effect on the loading capacity of HAuNPs. The dyes showed that loading is possible. Methyl Orange loaded the highest in concentration, while Acid Orange 5 was bound stronger to the HAuNPs. Chrysione Resorcinol did not load any dye to the HAuNPs. The trade off is good binding vs higher concentration of dye loading.

Introduction:

Cancer, characterized by the uncontrollable proliferation of defective or mutated cells in the body, is a heterogeneous and frequently detrimental disease [1-5]. Cancer has great effects on the personal lives of the individuals affected as well as those who know the individual [1]. There are currently more than 200 types of cancers, most of which have no cure [1]. For cancers, there are vast treatments being studied. Cancer currently has surgery, chemotherapy, radiation therapy, target therapy, nanoparticles, and other new technologies that are utilized to eliminate and hopefully cure cancer [1].

Targeted therapy is one of the many treatments available for cancer [1, 2]. Target therapy targets specific molecules or pathways that are involved in the growth and spread of the cancer cells [2, 3]. Different types of target therapies are designed to stop the uncontrolled proliferation that allow cancer cells to thrive, while minimizing the potential damage to unaffected, healthy cells [2, 3]. Targeted therapies have been developed for various types of cancers and have shown improvement and the potential for an effective treatment option [2, 3]. Among these target therapies, options of target therapy in combination with nanotechnology have much promise and can be used to help develop a drug for cancer treatment [4, 5].

Nanoparticles (NP) that are best for drug delivery systems are categorized as hollow nanoshells and nanocapsules, however liposomes and micelles are also used for drug delivery [6] (Figure 1).

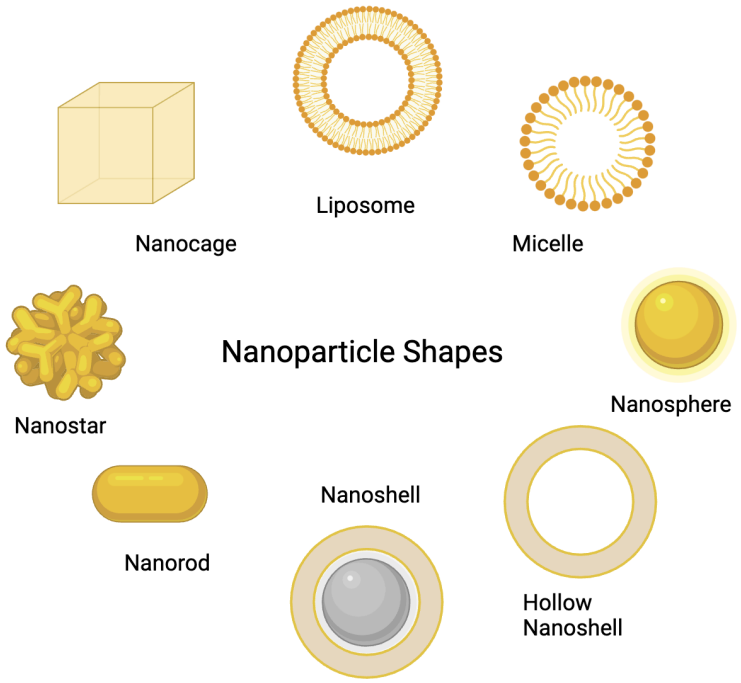

Figure 1. The different shapes that hollow gold nanoparticles can form.

Hollow gold nanoparticles (HAuNPs) are better for drug delivery use due to their surface to volume ratio and high permeability [7,18]. HAuNPs are made of gold, but instead of being solid gold they have an inner cavity that is hollow [7,18]. There are many different forms of nanoparticles, as seen in Figure 1, but the most ideal shape for drug delivery is hollow gold nanoshells [7,18]. Hollow nanoshells are the most desirable due to the ability to have drugs loaded into the cavaity as opposed to binding to the surface of the nanoparticle [7-12]. Loading drugs into the nanoparticles is ideal to ensure that the drug reaches its intended location inside the patient's body [13-15]. Once the nanoparticle reaches its intended site of infection, the drug payload is released upon interacting with the cancer cells [13-15]. The structures and properties of NPs have made them a great candidate for bypassing external barriers to enter cellular and subcellular locations within the body [19 20]. Each nanoparticle has a diameter that ranges from 1 nm - 100 nm due to the clusters or a large number of atoms that form the nanoparticle [19, 20, 6]. If the drug is

bound to the outside of the nanoparticle there is a higher chance for disassociation in the body prior to reaching its intended target; therefore, the treatment will be less successful. Studies suggest that the diameter of these nanoparticles allow for endocytosis and direct translocation for entry into cellular and subcellular locations [21-24].

Even though hollow nanoparticles are a promising new direction for target cancer therapy, little is known about the required characteristics of a drug molecule for efficient loading into the NP. According to *You et al.,* hollow gold nanoparticles were used to load Doxorubicin, a chemotherapy drug into NPs for use as a potential target therapy treatment [16]. The FDA has approved Doxorubicin to be used in combination with NPs for clinical trials [17]. Another drug, Cisplatin has been successfully used according to *Xiong et al.,* for NP target therapy [15]. Although these studies have shown great success in loading a drug molecule into a hollow NP, there can be no clear generalizations made since the conditions and NP characteristics were different for both of these studies. Additionally, *Dung et al.* determined that solid gold nanoparticles can have a peak in the NIR range from 600 -1000 nm which is best for penetration of IR light through the blood and tissues in the body [57]. The penetration of IR light allows the dye that is absorbed into the NP to be released into the body [58]. This is done through a NIR laser which excites the NP and initiates a photoreaction that forces the NP to release the drug [58].

This study aims to look at the loading efficiency of a series of dye molecules to mimic a drug with different bulk and polarity while keeping the nanoparticle characteristics and loading conditions constant throughout dye loading to determine if hollow gold nanoparticles have a loading capacity. This study will determine if there is a limit on the amount of a “drug” molecule that can be sequestered on (or in) the nanoparticle for target cancer therapy treatments.

The type of NP used depends on the application of the NP and the starting materials needed to create NPs. NPs are broken down into two categories: metal oxide/polymers NPs and metal/hollow NPs. Metal oxide NPs are used as sensors and some drug delivery [31,32]. Metal oxide NPs are typically nanospheres, nanorods, and nanocages [32]. The benefit of metal oxide NPs are the shapes that are created. The shapes are relatively nontoxic to cells, but the size is very hard to control and maintain with these procedures. Metal oxide NPs are created from the top-down methods which are very hard to maintain control over the output product size [31]. Metal and hollow NPs are hollow nanoshells, nanoshells, and nanorods which are used for drug therapy, cancer treatments, and biosensors [33]. For target cancer therapy in combination with drug delivery, the best NP are the hollow NPs. The reason is because hollow NPs are produced from bottom-up methods which use molecules in liquid, gas, or solid phases to form these nanoparticles [25]. These procedures are easier to use and the size, shape, and porosity of the hollow NPs are easily controlled in bottom-up methods [25]. The only downside to using hollow NPs is that there is not much research and the drug may only bind to the shell of the NP rather than going inside the NP [33].

The size, shape, and porosity of the nanoparticles are controlled by different synthetic techniques used to produce NPs. Micelles, liposomes, nanospheres, and nanocages are made from different starting materials than the nanostars, nanorods, and nanoshells [25]. The micelles, liposomes, nanospheres, and nanocages are processed by breaking down solid materials into the nanoparticles, this mechanism is commonly referred to as top-down [25].

Multiple studies have shown that the smaller nanoparticles are more toxic [26-29]. The studies looked at nanoparticles with various sizes, 2 nm, 15 nm, 45 nm, and 100 nm [26-29]. Other studies have been conducted to determine that nanoparticles that have a diameter of around 50 -

100 nm have the best cellular uptake. In these studies NPs with a 45 nm diameter had the most efficient uptake while larger diameters have smaller diffusion rates, but stronger interactions [26]. A study done by *Chithrani et al.* in 2006 examined AgNPs with diameter sizes of 5, 50, and 74 nm [30]. The study exposed cells to these AgNPs and they noted that 50 nm had the highest uptake, followed by 14 nm, and the 74 nm had the lowest cellular uptake [30]. The NPs with a size of 1.4 nm or less noted cytotoxic effects, while 50-100 nm had no cytotoxic effects [26] (Figure 2). Thus nanoparticles with a diameter of 50 nm - 100 nm exhibit the best size range for a drug delivery system.

Figure 2 discusses findings about how NPs' size affects the uptake processes within cells. Smaller NPs of less than 1.4 nm have been shown to be cytotoxic [26]. Depending on the cell line and NPs' material, medium sized (50 - 100 nm) NPs can be absorbed by diffusion, while larger NPs (150-500 nm) may be ingested by clathrin-mediated endocytosis [26]. Regarding gold NPs of large sizes, no cytotoxic effects have been found. It should be noted that uptake is influenced by both the NPs' materials and the cell line used.

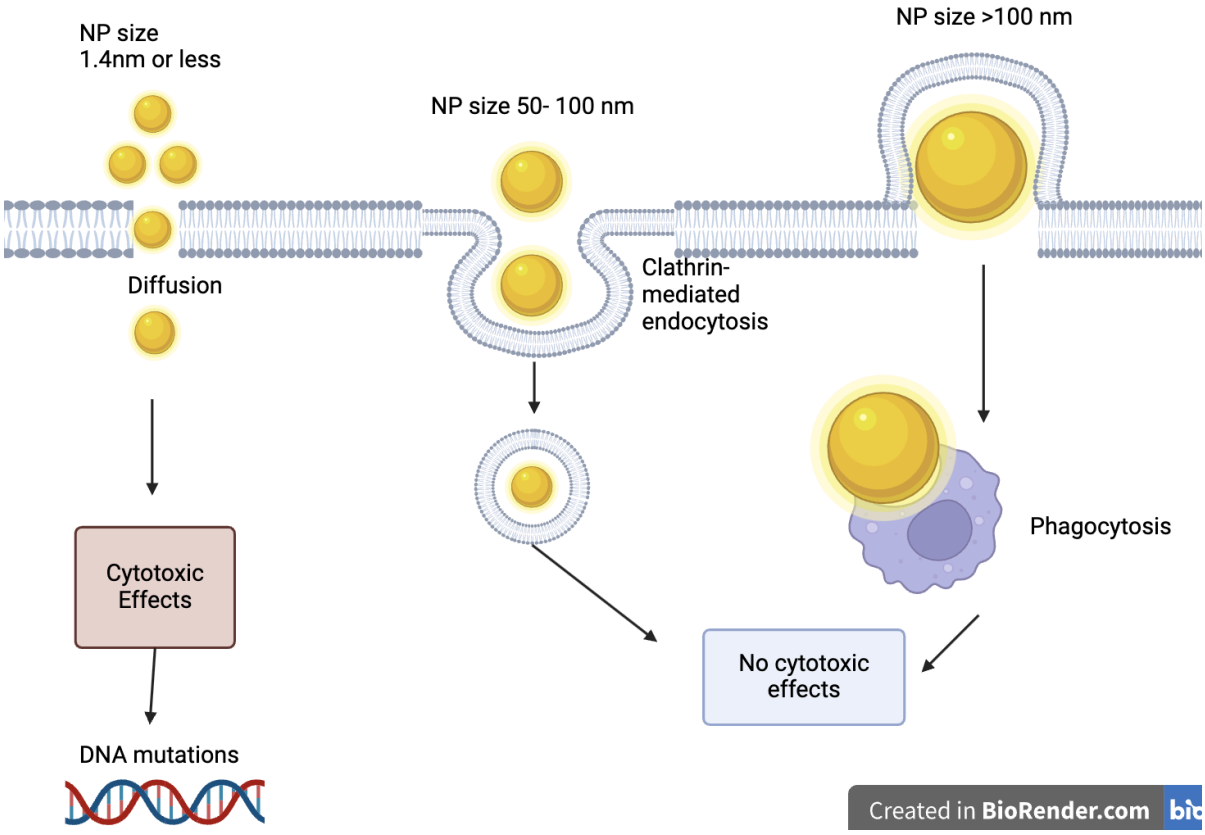

Figure 2. The diameter of the nanospheres has an impact on cellular uptake once the NP enters the cell.

Not only does the diameter affect cytotoxic activity, but the shape plays an important role in cellular uptake and cytotoxic activity as well. Nanoparticles with different shapes exhibit varying uptake rates and pathways by cells [26]. Nanospheres, stars, and hollow shells have shown higher uptake rates compared to nanocages and nanorods [26]. Shape also affects the pathways used to enter a cell. Different shapes may prefer to enter via endocytosis or phagocytosis [26].

Nanoparticles can be made of silver, gold, or even copper [6,35]. Copper NPs are less reactive and more stable when in contact with the air than in the body, while silver NPs are easily absorbed in the respiratory and digestive systems [35]. However, when looking at the potential toxicity of NPs, while gold nanoparticles exhibit small toxicity, silver nanoparticles are more toxic in higher concentrations [34,35]. Silver nanoparticles (AgNP) are toxic due to the ionic form of

silver (Ag+) that is in concentrations with the AgNPs [34,35]. These silver ions inhibit the effects of ATPase causing an imbalance of Na+/K+ ions [34,35]. Thus, the most desired NPs for a drug delivery system are hollow gold nanoparticles [7-12].

Synthesis of HAuNPs are most commonly done using galvanic replacement reactions using another nanoparticle as a template [34-37]. The most common procedure to synthesize HAuNPs uses AgNPs as a sacrificial template [7-9,36]. First AgNPs must be synthesized and then gold is added to the solution of the AgNPs [7-9,36] (Reaction a or b).

$$AgNO_3 + PVP \xrightarrow{\text{Ethylene Glycol}} Ag_{(s)} + NO_3^- \quad \text{(a)}$$

$$2\,Ag^+_{(aq)} + 2\,BH^-_{4\,(aq)} \longrightarrow 2\,Ag^0_{(aq)} + B(OH)_{3\,(aq)} + H_{2\,(g)} \quad \text{(b)}$$

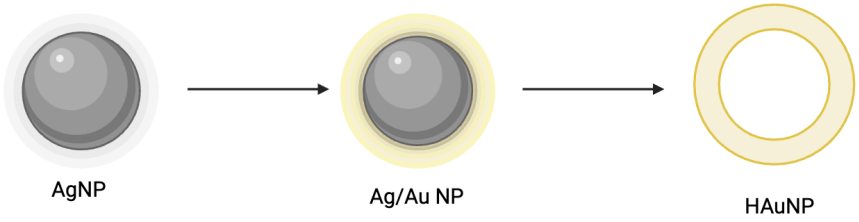

$$3\,Ag_{(s)} + AuCl^-_{4\,(aq)} \longrightarrow Au_{(s)} + 3\,Ag^+_{(aq)} + 4\,Cl^-_{(aq)} \quad \text{(c)}$$

$$3\,Ag \longrightarrow 3\,Ag^+ + 3\,e^- \quad \text{Anode reaction}$$

$$AuCl^-_4 + 3\,e^- \longrightarrow Au + 4\,Cl^- \quad \text{Cathode reaction}$$

The gold oxidized Ag to Ag+ which is dissolved in solution (Reaction c). In this process, Ag is replaced by Au. The reaction is dependent on the different reduction potentials of the Ag and Au [6,7,18,37]. The gold reduction potential from the reduction of $HAuCl_4$ to Au is higher while the Ag reduction potential of $AgNO_3$ to Ag is lower than the gold reduction potential [7-9,37]. The reduction potentials explain how the chloroauric acid ($AuCl_4$) reduces the silver to make HAuNPs. The reaction that occurs between the $HAuCl_4$ and the $AgNO_3$ creates a gold shell around the previous AgNPs which creates a hollow nanoshell (Equation c) [7-9,36]. The reaction uses a ratio of 3:1 (3 silver: 1 gold), for every gold atom used 3 silver ions are displaced from the NP until a solid shell of gold is formed [7-9,36].

AgNP synthesis is done using a reducing agent [11]. The strength of the reducing agent affects the synthesis of the NPs [11]. Sodium borohydride ($NaBH_4$) is a strong reducing agent which can positively reduce the silver ions (Ag+) to a neutral charges silver ion (Ag^0) as seen in Reaction e [11]. Thus, sodium borohydride is able to influence the shape, size, and stability of the AgNPs [11]. However, because sodium borohydride is in excess in this process of making AgNPs for the galvanic reduction reaction, the sodium borohydride needs to be quenched [38]. The quenching of the $NaBH_4$ is due to a reaction which calls for $NaBH_4$ to be in excess [38] (See Reaction d and e).

$$NaBH_{4\,(s)} + H_2O_{(aq)} \rightarrow Na^+_{(aq)} + BH^-_{4\,(aq)} + H_2O_{(aq)} \quad \text{(d)}$$

$$5\,BH^-_{4\,(aq)} + H^+_{(aq)} \rightarrow 6\,H_{2\,(g)} + B_2H_{6\,(g)} + B(OH)_{3\,(aq)} \quad \text{(e)}$$

If there is excess of $NaBH_4$, it will reduce the gold in $HAuCl_4$ before the silver can [38]. The excess will result in a solution mixture of both silver and gold NPs rather than the Au replacing all the silver leaving only gold NPs [38].

When synthesizing NPs, a capping agent can be used to ensure the stability of the NP created (Seen in Figure 3) [9]. A capping agent can be used with a reducing agent or act as the reducing agent in reactions [11]. Capping agents allow for better binding affinity, flexibility, and more stability of the surface of NPs [9]. Capping agents are an amphiphilic molecule that have a polar head and a nonpolar tail. The capping agents align with the nonpolar end on the surface of the NP and the polar end interacts with the outside [10,39]. This is true since the capping agent in this study is non-polar and the NPs are in solution of polar water. The capping agent can be covalently bound to a NP in Figure 3.

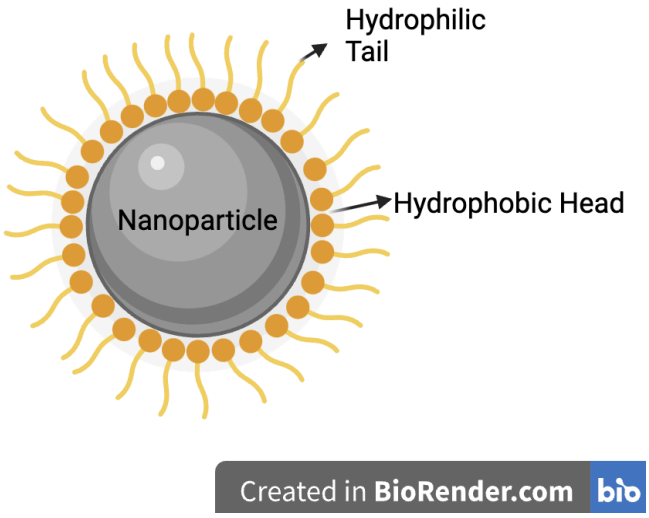

Figure 3. A capping agent is covalently bound to a nanoparticle

Capping agents help to "stabilize" the particles while in a solution [40]. The capping agent properties determine the intake of NPs in cells as well as preventing the particles from aggregating and forming large clusters that drop out of solution [9,40]. The charges of the capping

agent and their interactions with the surface of the AuNPs determine the intermolecular forces (IMFs) between particles within the solution [40]. The main IMF that is attributed to this is Van der Waals forces [40]. When the particles are in solution without a capping agent, Van der Waals will force the particles to come together and aggregate to form large clusters of NPs [40]. By using a capping agent, the NP is surrounded by either a charged capping agent or a bulky capping agent. This prevents the NPs from colliding with each other due to repulsion of the charge of the capping agent or the overall bulk of the capping agent [40] (Figure 4). The interactions between the capping agents and the NPs are what helps to "stabilize" or prevent the NPs from clumping while in solution to allow for a higher potential for drug target therapy.

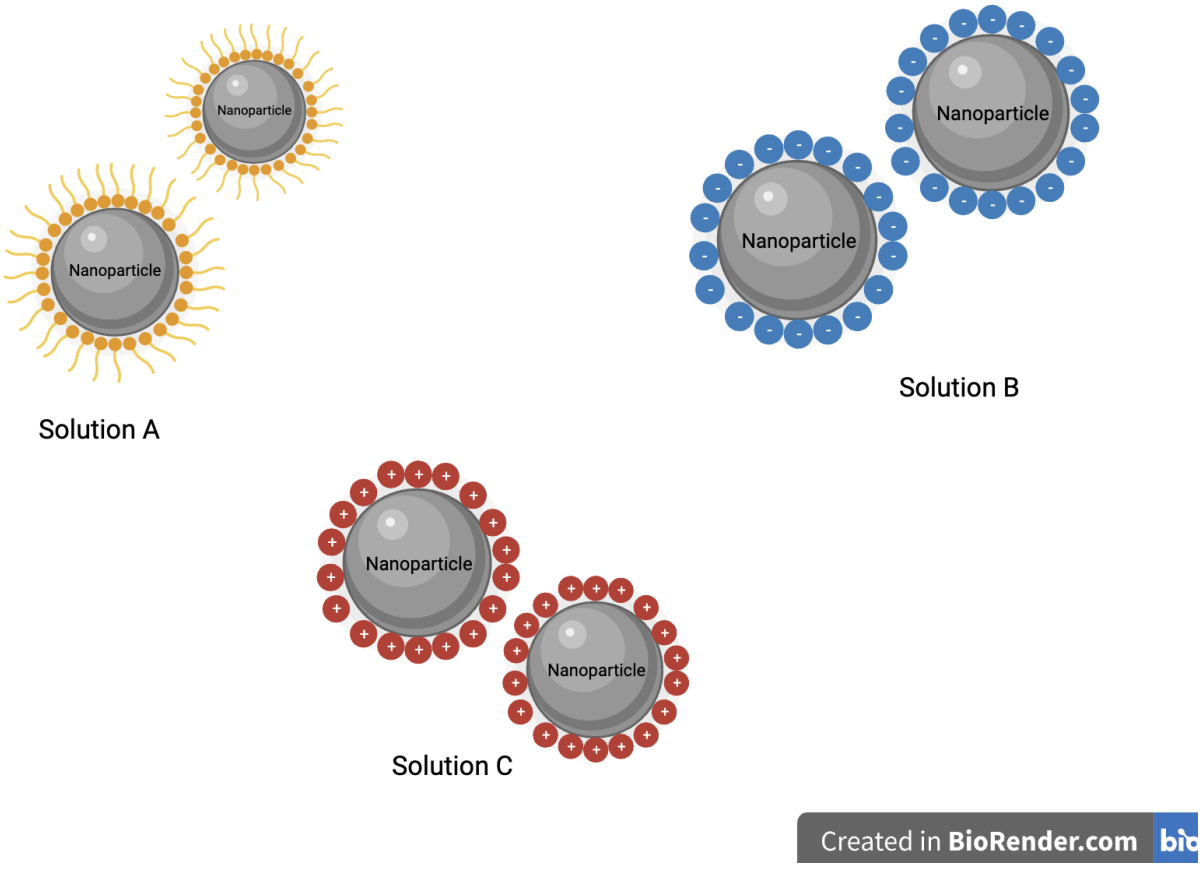

Figure 4. IMF aggregation: Repulsions and charges of capping agents on nanoparticles within solution. Solution A is an example of PVP capped nanoparticles. Solution B is an example of citrate ion capped nanoparticles. Solution C is an example of CTAB capped nanoparticles.

Typically for AuNPs, the most common capping agents used are Cetyltrimethylammonium bromide (CTAB), Poly(vinyl pyrrolidone) (PVP), and citrate ions (Diagram 1) [9].



(1) (2) (3)

Diagram 1. Structures shown of the three common capping agents for comparison and visualization, (1) Citrate ion. (2) Poly(vinyl pyrrolidone). (3) CTAB

Citrate capped gold has been shown in research that the high pH is toxic to the liver as a result of citrate binding with calcium in the body, thus causing hypocalcemia [9]. CTAB is very toxic to the liver cells due to the molecules forming smaller and less stable micelles in liquid [8,39]. PVP is a capping agent that helps with the sizing of the product NPs [39]. Although PVP is the most commonly used, this study uses borohydride from sodium borohydride (See reaction f). A capping agent interacts with both the surface of the particles and the solvent. Since the solvent in this study is water, the capping agent needs to be a Lewis base to bind to the Ag on the surface of the particle and interact well with water [39, 60] . In this case, the BH_4 from $NaBH_4$ acts as the capping agent in a water solution. Since the water is polar, and $NaBH_4$ is ionically bound, it dissociates into Na^+ and BH_4 where Na^+ is a spectator ion and BH_4 is what reduces and caps the particles (See reaction g).

$$2\,AgNO_{3\,(aq)} + 2\,Na^{+} + 2BH_4^{-} \rightarrow 2\,Ag_{(s)} + H_2 + B_2H_6 + 2\,NaNO_3 \qquad \text{(g)}$$

Drug loading is done with hollow nanoparticles (HNPs) by adding the drug molecule to the NPs while the solution and then either sonicating, heating, or stirring the mixture to force the drug molecules into the inner cavity [13-15]. Dyes are used for the ease of measuring loading capacity of the HAuNPs. The study is investigating the loading capacity of the HAuNPs. The electrostatic interactions between the dye and the particle could affect the loading capacity of the drug into the hollow cavity of the HAuNPs. There are two loading capacities at play, the dye in solution and the dye on/in the particle [16,23,41,42]. When loading the dye into the NP, the dye is added to the HAuNPs in solution, known as the concentration of dye in solution. The dye that is not in solution is either in the cavity of the HAuNP or bound to the surface of the particle, this is known as the loading capacity on/in the particle. Each of these capacities are found using UV-vis spectroscopy. Using a UV-vis spectrum can determine the loading capacity of dye in solution and in/on the particle after combining the dye and particles in solution together.

When using dyes for loading studies with nanoparticles, a most commonly used dye was considered. *Sollis* used Alizarin red S dye to determine that there is multilayering of the dye on the surface of the NPs [42]. For that study, Alizarin red S was chosen for its pH sensitive color changes [42]. The pH changes allowed for easy monitoring of the pH environment [42]. This multilayering of the dye suggests that some dye binding may be dependent on the concentrations used [42]. This multilayering can also suggest that alizarin red S was successfully absorbed into the HAuNPs [42]. Since *Sollis* was able to determine multilayering of dyes on HAuNPs surface, then the dyes used in this study may also exhibit the same interactions.

The dyes used in this study were chosen based on structure, bulk, polarity, and weight. The three dye chosen were Methyl Orange, Acid Orange 5, and Chrysione Resorcinol (Diagram 2). The three dyes were chosen first based on their molecular weights. Each dye is around 300

g/mol to prevent secretion in the liver and is soluble [44]. The solubility of the dye is important when choosing a dye because research shows that it increases the encapsulation of the dye within the particle [45-49]. By choosing a dye that is soluble in water (high solubility), there is an increased chance that the drug will be absorbed into the particle [45-49]. The dye's structure also has an amine group that can be protonated based on the pH environment, which is a distinguishing feature of most common cancer drugs [42].

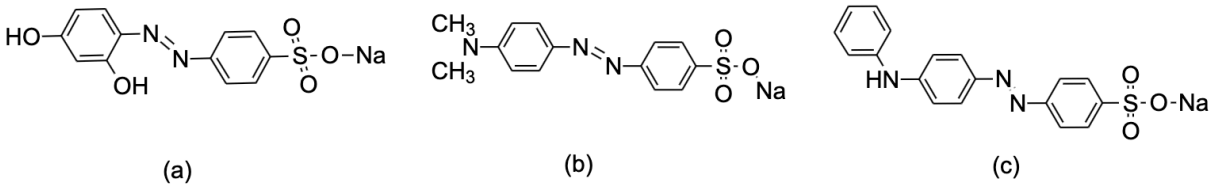

Diagram 2. Comparison of dyes (a) Chrysoine Resorcinol (b) Methyl Orange (c) Acid Orange 5

Methyl Orange was chosen as the starting structure (**b**) for the loading studies. Methyl Orange has a molecular weight of 327.32 g/mol, a pKa of 3.1-4.4, and is soluble in water [50]. At a pH of 7, the solution is more basic than the pKa of the dye (about 3.5) which results in a charge on one of the nitrogens in the N=N (Diagram 3 and 4). The structure of Methyl Orange contains the SO_3Na and the phenyl groups, but has two open methyls at the end of it. This dye serves almost as a "control" for the other two dyes picked.

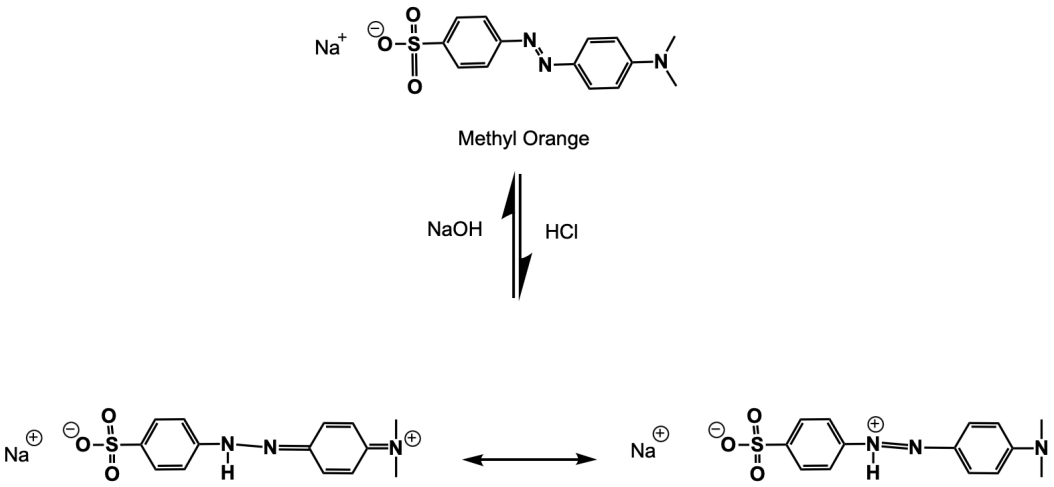

Diagram 3. Acidic and basic form of Methyl Orange. The acidic form is on the bottom and the basic form is on the top.

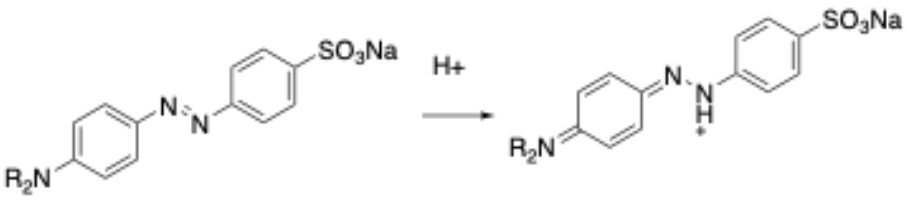

Diagram 4. Shows the protonation of the dyes to result in a neutral charge due to pKa.

To determine if polarity has an effect on the loading capacity, the dye Chrysoine Resorcinol was picked. Chrysoine Resorcinol differs from Methyl Orange in polarity. Chrysoine Resorcinol has a molecular weight of 317.27 g/mol, pKa = 11.9 and 3 -4, and is partially soluble in water [47]. The structural difference between Chrysione Resorcinol and Methyl Orange is a result of Chrysoine Resorcinol being slightly more polar than Methyl Orange. The polarity is different because Chrysoine Resorcinol has two OH groups attached to the phenyl group as opposed to two methyl groups which results in more polarity (Diagram 2 (a)). The charge on the dye here is negative due to the pH being lower than the pKa of 11.9 which results in deprotonation of one of the OH groups and protonation of one of the nitrogens from the N=N (See Diagram 4).

To determine if size has an effect on the loading capacity, the dye Acid Orange 5 was picked. Acid Orange 5 differs from Methyl Orange in structure. Acid Orange 5 has a pKa of 2.3, but is more bulky compared to Methyl Orange [51]. This results in a slightly higher molecular weight at about 375.4 g/mol [51]. The overall difference between this dye and Methyl Orange is the third phenyl group instead of the two methyl groups at the end of the molecule (Diagram 2. c). The charge on this dye is like methyl orange due to the pH of 7 being much higher than its pKa of 2.3 (Diagram 5).

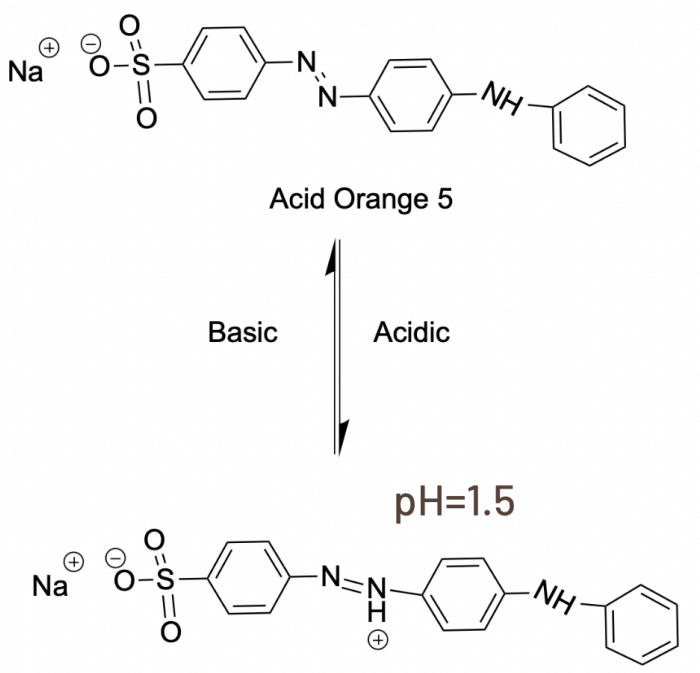

Diagram 5. Acidic and Basic forms of Acid Orange 5

Zeta potentials measure the potential energy of the "slipping plane" around a particle in suspension [52]. The potential represents the amount of work needed to replace a charge on the surface of the particle and is important in determining the stability of the particles in solution [52]. A high zeta potential represents better stability as it forms a barrier between particles, thus influencing IMFs and electrostatic repulsions [52]. A high potential impacts the absorption of dyes

onto/into the NP [52]. The zeta potential influences the attraction of the dye, as well as the dipole-dipole, and the hydrogen bonding interactions between the dye and the surface of the particle [52]. Studies have shown that HAuNPs have a negative zeta potential depending on the capping agent used and the size of the HAuNP as well as other ions found in the solution [42]. Since the particles have a low stability alone, they need capping agents to form strong IMFs between the particle and the solvent used in the synthesis of NPs [42,52,53].

When a dye is loaded into the NP solution, the IMFs and repulsions are at play to determine how much of the dye goes in or on the particle. Chrysione Resorcinol is expected to load less than the Methyl Orange as a result of the dye's stronger interaction with the water in solution rather than interacting with the Au atoms at the surface of the NPs. The higher polarity would result in less binding interactions with the surface of the HAuNP and disassociate more in water due to the IMFs between water and polar molecules. Acid Orange 5 dye is expected to load less into the nanoparticle due to the larger size of the dye molecule compared to Methyl Orange since Acid Orange 5 will take up more space in/on the NP, so less will fit into/onto the NP. Finally, the Methyl Orange is expected to load the most into the HAuNPs since it is the "contol" in this study.

Materials and Methods:

Materials.

Reagent Silver Nitrate (Acros Organics, 99+%), 10.85 mM Aqueous Chloroauric Acid ($HAuCl_4$), Poly(Vinyl Pyrrolidone) (PVP, M_w=55,000 repeating units, Aldrich), Reagent Anhydrous Ethylene Glycol (99%, Aldrich). 20mM solution of Sodium borohydride ($NaBH_4$), 0.1 M Hydrochloric Acid (HCl), and 0.1 M Sodium Hydroxide (NaOH).

Synthesis of Hollow Gold Nanoparticles from Sodium Borohydride.

This synthesis was adapted from a procedure to make AgNP surfaces. A stock solution of 10mM Silver Nitrate and 20mM solution of Sodium Borohydride were made using ultrapure water. Ultrapure water was measured out to 30 mL and combined with 1 mL of the stock $NaBH_4$ solution. The solution was mixed fairly fast without splashing the solution. While the solution was still stirring, 1 mL of the $AgNO_3$ solution was added slowly by drops to the mixture. The solution turned a marigold yellow color. The solution was mixed for 20 minutes to ensure the reaction was complete. After 0.1M HCl was added in drops while the pH was tested after each drop till the solution reached a pH of 3. Once the solution reached a pH of 3, the solution was raised back to a pH of 7 using 0.1 M NaOH. These products, silver colloids, were confirmed using UV-Vis spectroscopy.

The silver colloids were then measured out (3mL) and began stirring rapidly. A 200 uL aliquot of 10.85 mM solution of $HAuCl_4$ was added slowly by drops to the mixing silver colloids. The solution turned clear navy blue. The final products, HAuNP, were confirmed using UV-Vis spectroscopy.

Dye Beer's Law Calibration.

Methyl Orange, Acid Orange 5, and Chrysione Resorcinol were each used separately to plot a Beer's Law Curve. Each dye was used to create various concentrations from 0 - 152 uM for methyl orange, 0 - 133 uM for acid orange 5, and 0 - 158 uM for chrysione resorcinol. Each concentration for all the dyes were made by adding the correct grams of dye to 500 mL of ultrapure water. The concentrations were then collected and analyzed using a UV-vis spectrometer. Every absorbance was measured at a wavelength of 470 nm.

Loading Dyes to HAuNPs.

Chrysoine Resorcinol, Methyl Orange, and Acid Orange 5 dyes were used and combined with HAuNPs. Each study was done by starting with different concentrations of HAuNP solution, 5% (v/v), 15% (v/v), and 75% (v/v). For a given dye, four different dye concentrations were combined with each concentration of HAuNPs. This was repeated for each of the three dyes. Three replicates of each combination were analyzed for a total of 108 samples. Two groups of samples were sonicated for 2 hours, and the last sample is the control where they are not sonicated and allowed 2 days to absorb the dye. All samples were then centrifuged for 15 minutes at 10,000 rpm. The supernatant was collected from each solution after centrifuging. One sample set and the "controls" were washed three times and the other was not. Washing was done by collecting all the supernatants and combining them into a 10 mL volumetric flask. Then the absorbance of the supernatant is measured using a UV-vis spectrophotometer and analyzed at a wavelength of 470 nm.

Instrumentation.

Hollow gold nanoparticles were confirmed within solution by using UV-vis spectroscopy. Each sample was run in room temperature conditions on a Olis-Carey 8453 UV-vis

spectrophotometer. The scans were run from 400 nm to 1100 nm to capture the expected NIR peak of the HAuNPs. A quartz cuvette was used to perform the test on each sample.

Results and Discussion:

Silver Nanoparticle Synthesis:

The synthesis for AgNPs relies on the reduction of a sacrificial template, Ag (See footnote [1]).The sodium borohydride ($NaBH_4$) synthesis used $NaBH_4$ as both the reducing and capping agent. The sodium borohydride is used in large quantities for this study first as the reducing agent and then as the capping agent. $NaBH_4$ is able to reduce the silver nitrate to $NaNO_3$ salt and silver nanoparticles [59] (see reaction g). While the mixture is stirred, the reaction finishes by allowing BH_4 to work as the capping agent as the Ag is reduced in solution. The BH_4^- is absorbed on the surface of the particles creating a slight negative charge on the surface, thus preventing aggregation in solution and creating stable AgNPs [59] (See Reaction g).

$$2\,AgNO_{3\,(aq)} + 2\,Na^{+} + 2BH_4^{-} \rightarrow 2\,Ag_{(s)} + H_2 + B_2H_6 + 2\,NaNO_3 \qquad \text{(g)}$$

Silver nanoparticles have optical properties that can be analyzed using localized surface plasmon resonance (LSPR). AgNPs are efficient at scattering and interacting with light due to the electrons on the metal (Ag) surface that oscillate when exposed to light at specific wavelengths [60]. The light has the same frequency of the electron oscillations at the surface of the particle causing the AgNPs to scatter off the particles most strongly. The wavelengths are scattered out of the light beam and are not detected at the detector of the UV-vis spectrometer. Thus the incident light beam looks like an absorbance since those wavelengths are missing from the incident light.

[1] The two different syntheses, PVP (Reaction a) and Sodium Borohydride (Reaction b), were used to make silver nanoparticles to be used in a galvanic reduction reaction (Reaction c) to make HAuNPs. The sodium borohydride had a much simpler approach than the PVP synthesis for the nanoparticles. The PVP was unable to yield any AgNPs.

The absorbance frequency is known to be around 400 nm [60]. Thus UV-vis spectrum which records LSPR can be used to confirm the presence of AgNPs in a solution. The UV-vis spectrum of the hydride capped silver nanoparticles (Figure 5) agrees with the literature and shows a single resonance peak around 410 nm, which represents AgNPs. *Khatoon et al.* identified silver nanoparticles that were reduced by sodium borohydride with a resonance peak between 390 nm and 430 nm [11]. These silver nanoparticles were prepared for $HAuCl_4$ reduction.

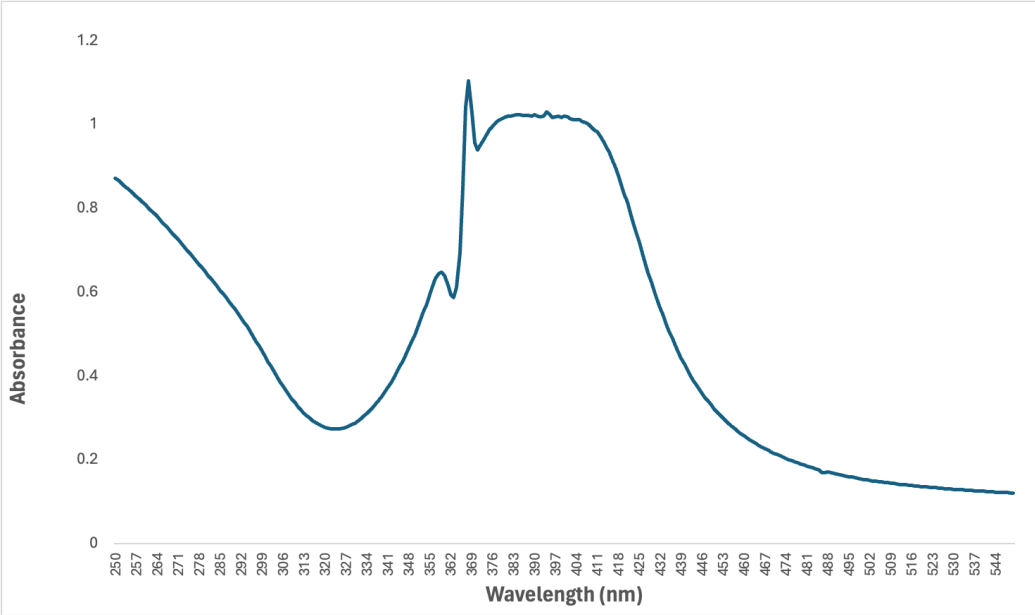

Figure 5. The absorbance spectrum for AgNPs from $NaBH_4$ synthesis. The maximum wavelength is at 410 nm, confirming silver nanoparticles.

Hollow Gold Nanoparticle Synthesis:

Once the silver nanoparticles were confirmed using UV-Vis, they were able to be used to make hollow gold nanoparticles. Using the prepared silver nanoparticles, 10mM solution of $HAuCl_4$ was added to the solution slowly by drops which resulted in the formation of hollow gold nanoparticles. When chloroauric acid is added to the silver nanoparticles, the gold grows small particles and these gold particles form a ring around the silver colloid. The gold and silver

are able to freely float around the surface of the silver colloid until all the silver is reduced completely creating a hollow gold nanoparticle.

When analyzing the HAuNPs using SEM imaging, the particles were difficult to see and capture an image. However, like AgNPs, hollow gold nanoparticles have the ability to be detected by light [60]. HAuNPs are also detected using LSPR and each peak indicates a different structure of nanoparticles [60]. The UV-vis spectrum for the HAuNPs (Figure 6) agrees with the literature where a single peak is seen in the NIR (Near Infrared Light) range at about 980 nm. *Wang et al.* found that their hollow gold nanoparticles had a peak around 957 nm by synthesis using 3-aminopropyltriethoxysilane as their capping agent instead of sodium borohydride [36].

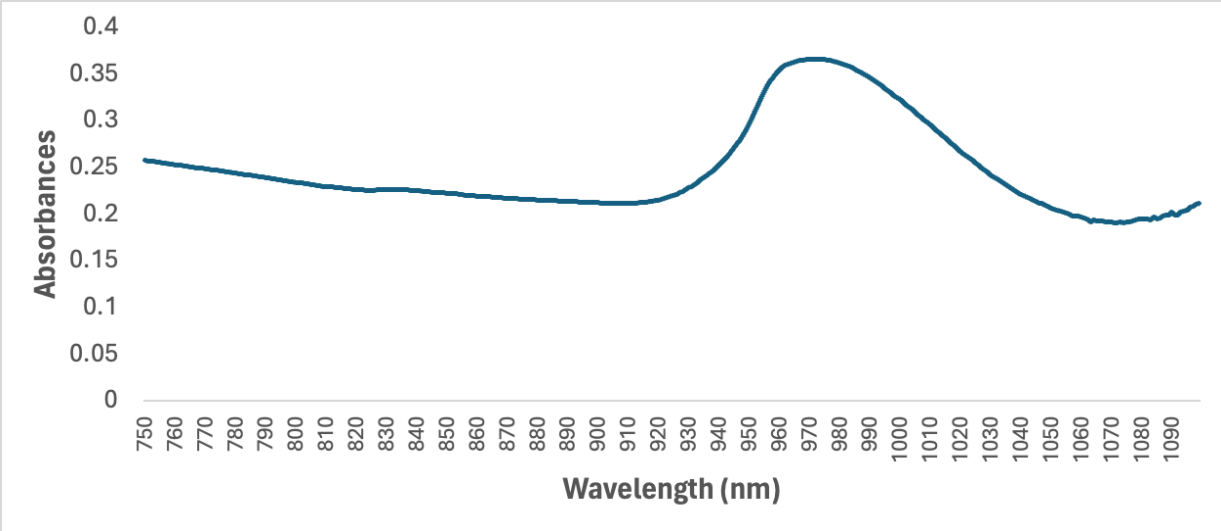

Figure 6. The absorbance spectrum of HAuNPs. The maximum wavelength is at 980 nm, confirming hollow gold nanoparticles.

Although the easier synthesis of the HAuNPs seem to confirm the presence of hollow gold nanoparticles, SEM imaging was done to ensure that the particles are present and the correct shape and size. SEM imaging was unable to capture a clear image of particles on the nanoparticle size scale. This was due to the charging of the electrons on the surface of the

particle. The SEM was charging the atoms creating too much light for a clear picture of the NPs. Thus there are no SEM images to confirm with UV-Vis that HAuNPs were successfully created.

Loading Studies:

To further understand the loading capacity of HAuNP, the dyes Methyl Orange, Acid Orange 5, and Chrysione Resorcinol were loaded into the HAuNPs to mimic the use of drugs. Three beer's law calibration curves were created. The maximum wavelength absorbance was at 430 nm for Methyl Orange, 434 nm for Acid Orange 5, and 429 nm for Chrysione Resorcinol (Figures 7).

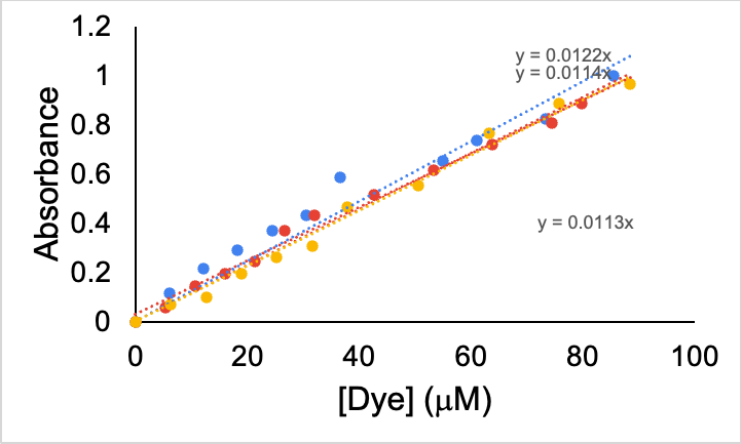

Figure 7. Beer's Law Calibration Curve. Methyl Orange is blue. Acid Orange 5 is red. Chrysione Resorcinol is yellow

The slope of the line for each curve give the concentration of each dye supernatant after centrifugation, C_{loaded}. The concentration of the dyes loaded into the HAuNPs were converted into moles of Methyl Orange, $n_{load\ Methyl\ Orange}$, moles of Acid Orange 5, $n_{load\ Acid\ Orange\ 5}$, and moles of Chrysione Resorcinol, $n_{load\ Chrsione\ Resorcinol}$. Coverage, Θ (moles of dye/grams of Au), is then determined to specify how much went inside the particle/on top of the particle. The moles

of dye loaded are divided by the mass of gold used during the synthesis. Figure 8 shows the coverage for each dye concentration at 5% and 15% HAuNP concentrations.

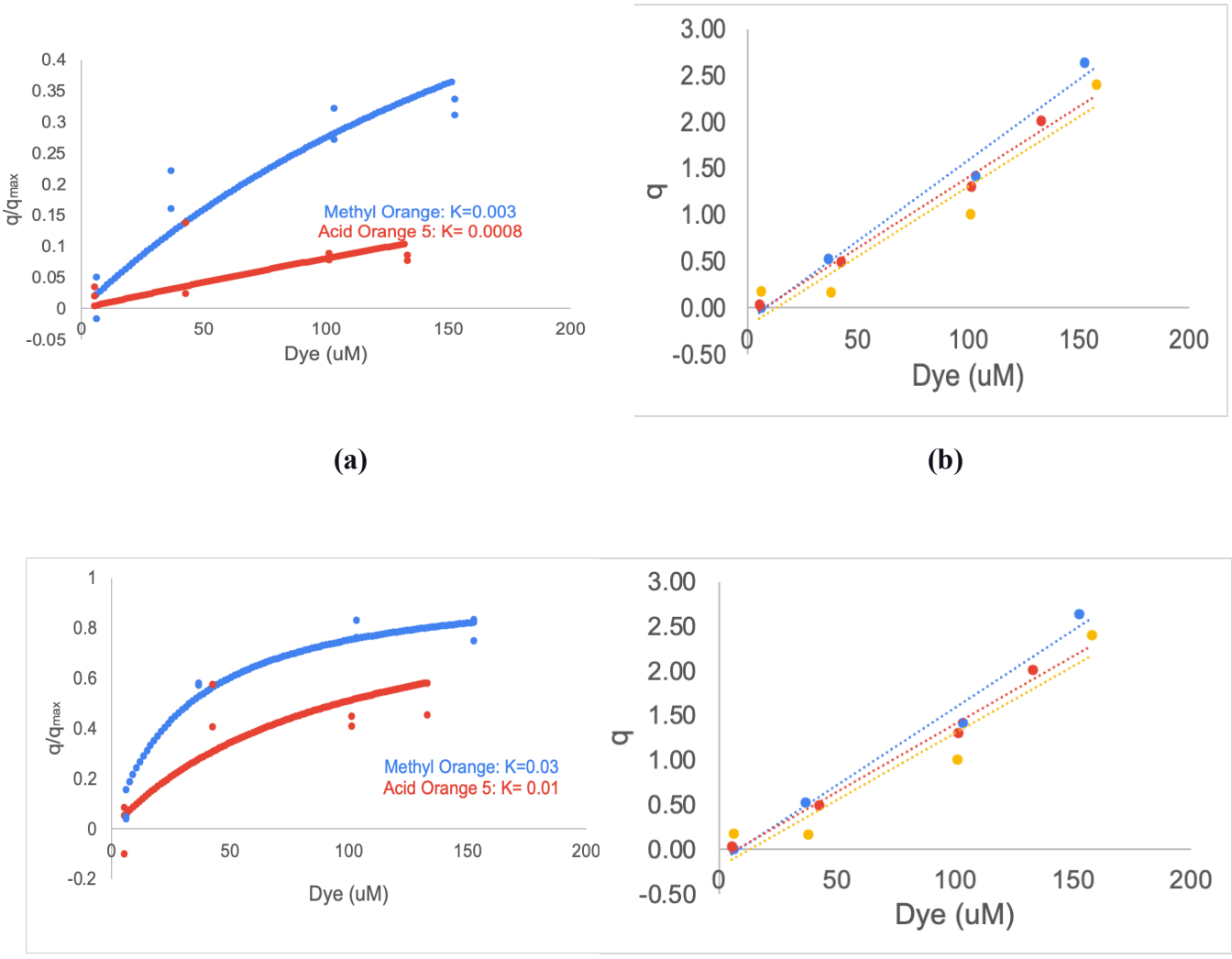

Figure 8. For each sample Methyl Orange is blue, Acid Orange 5 is Red, and Chrysione Resorcinol is yellow. A) Wash 5% (v/v) samples. B) No Wash 5% (v/v) samples. C) Wash 15% (v/v) samples. D) No Wash 15% (v/v) samples. Note the 75% samples are not shown here.

The coverage (Θ) values for each of these samples confirms that the dye was successfully loaded in/on the HAuNPs. However, Chrysione Resorcinol did not load any dye at all after

washing, while Methyl Orange and Acid Orange 5 only loaded at 5% and 15% HAuNP concentrations.

Since this system is a liquid-solid equilibrium system, the Langmuir Isotherm Theory can be applied to explain the absorption of solutes in solution across the solid nanoparticle surface. This theory can only be applied to this study if the following assumptions are made: there is a limited amount of binding sites for the dyes over the surface of each particle (q_{max}), each binding site has the same attraction to the dye, there are no interactions between each particle that is in solution, and the absorption of the dye into/onto the particle can be reversed [61 - 64]. The system used in this study is in equilibrium under the Langmuir isotherm theory (See reaction h).

$$Dye + Surface \leftrightarrow Surface * Dye \quad \text{(h)}$$

$$K = \frac{[Surface * Dye]}{[Dye][Surface]} \quad \text{(i)}$$

$$Surface = \Theta \; ; \quad Surface * Dye = 1 - \Theta \; ; \quad \text{(j)}$$

$$K\,[Dye]\,\Theta = 1 - \Theta \quad \Rightarrow \quad \Theta = \frac{K\,[Dye]}{(1 + K\,[Dye]\,)} \quad \text{(k)}$$

The equilibrium reaction is defined as Dye plus the surface is in equilibrium with the surface-dye complex [68] (Equation h). The equilibrium constant (K) can be found by products over reactants (Equation i). Since we need to determine the coverage of dye over the surface sites, we can define the surface as Θ, which represents the fraction of open surface sites [68]. If theta is open surface sites, 1-Θ is defined as the filled surface sites on the NP [68]. We can calculate the coverage ($\Theta = q/q_{max}$) using mass of gold per number of surface sites [68] (Equation k). By graphing q/q_{max} vs [Dye], the comparison of overall coverage can be made (Figure 9).

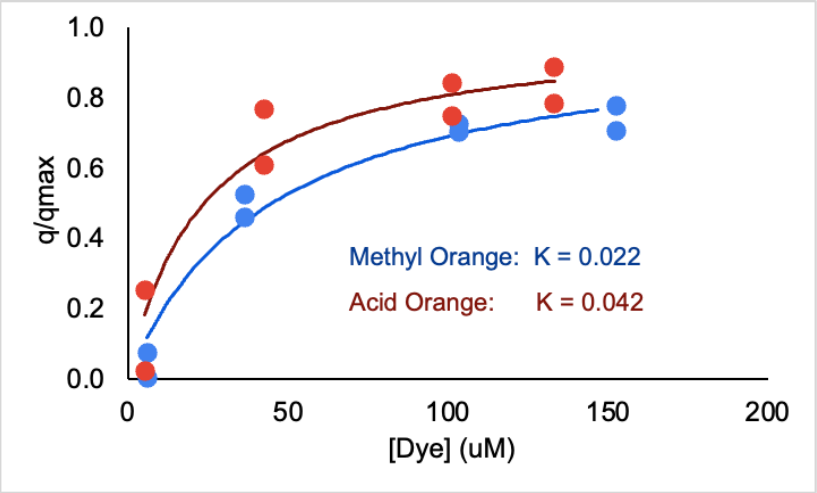

Figure 9. The Langmuir Model for Methyl Orange and Acid Orange 5.

The q_{max} is different for each concentration of HAuNP, but the coverage is the same for all the dyes. Different concentrations of HAuNPs were used with various concentrations of dye for each loading method used. The not washed samples had a much higher concentration of dye loaded in/on the HAuNPs. After washing, all the Chrysione Resorcinol was washed off as well as much of the Methyl Orange and Acid Orange 5 thus the smaller absorbance values. This may be a result of the dye interactions between themselves and the HAuNPs. The dyes are not very soluble in water and each dye has a lot of pi-pi stacking interactions with one another [69]. This results in dye aggregation on the surface site and the dye molecules binding to each other. The dye - dye interactions are weaker than the dye - particle interactions so when the particles were washed, the weakly bound dye molecules stacked on top of one another were removed. So after washing, the dye molecules that are left are strongly bound and interacting with the HAuNPs surface.

The difference between the two loading methods was that one set was washed while the other was not washed. The results of the study noted no significant differences on the coverage (Θ) recorded between the sonicated and not sonicated samples. This shows that there is not one

method that is the best for loading and that the dye composition did affect the binding to the surface of the particles. The wash was intended to wash off the excess dye bound to the surface of the particle, this shows that the dye had reached maximum loading capacity and excess bound dye was removed.

The equilibrium constant, K, for each of the dyes can be used to understand the loading of the dyes with the HAuNPs. Methyl Orange has a K value of 0.022 while Acid Orange has a K value of 0.042 and Chrysione Resorcinol did not have a K value at all. The data suggests that when loading dyes Acid Orange 5 is the best and Chrysione Resorcinol is the worst. The reason for this may be attributed to the physical and chemical properties of the dyes used in this study [65 - 67].

Methyl Orange and Acid Orange 5 are both classified as azo dye, but each have their own chemical structure [65-67]. Acid Orange 5's structure has the OH on the end of the phenyl group while methyl orange does not [65-67]. The nonpolar OH group is able to form strong IMFs with the surface of the HAuNPs [65-67]. This is evident with the acid orange 5 having a higher K value than Methyl Orange. These interactions must be promoting higher absorption of Acid Orange 5 into/onto the HAuNPs' surface when compared to Methyl Orange which is slightly more polar [51, 65-67].

The binding of the dye is not quite known. It is difficult to determine if the dyes are binding to the outside of the surface as well as entering the hollow cavity of the HAuNP. However, the way the molecules are bound to the surface of the dye can be predicted. Since all the dyes are classified as azo dyes, each dye has a flexible double bonded nitrogen (N=N) in their structure which allows for flexible movement of the dye [51, 65-67] . The double bonded nitrogen can rotate to form a cis structure of the dye when the dye is in solution as seen in Diagram 6.

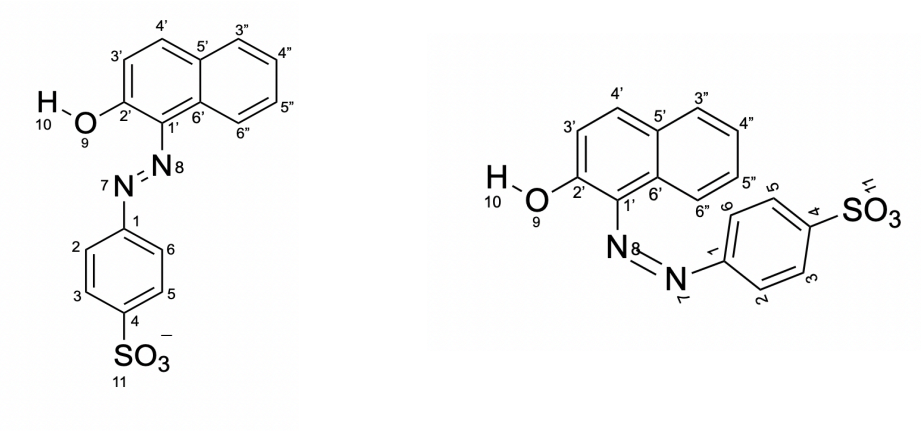

Diagram 6. Structure of Acid Orange 5 and its possible conformational structures

When the structure rotates it creates stress and hindrance on the molecule, therefore it is more likely that the molecule binds while in the trans conformation which is shown on the left in Diagram 6.

Although the K values indicate better binding for Acid Orange 5, the coverage (Θ) shows that Methyl Orange loaded more in concentrations than Acid Orange 5. The coverage for Acid Orange 5 was 0.6 (not washed) and 0.09 (washed) while Methyl Orange was 1.03 (not washed) and 0.5 (washed). Thus in terms of binding, Methyl Orange loaded more in concentration than Acid Orange 5. This can be attributed to the size of the dyes. Since Acid Orange 5's structure is larger (extra OH group), the dye takes up more space (binds to more surface sites) on the surface of the HAuNP resulting in less dye binding to the HAuNPs.

Overall, the higher loading efficiency of Acid Orange 5 onto/into the HAuNPs can be a result of a combination of factors. The structure and electrostatic interactions ultimately influence the absorption and equilibrium between the dye and HAuNPs. Thus the HAuNPs can have either stronger binding or high concentrations of the dye to bind on/in the particle. While the conclusion makes sense, there is not a ton of literature that is out to either support or deny

these findings, and it will require further research to understand the exact capacity of these HAuNPs.

Future Directions:

This project can be expanded in many different ways. One way would be to test more concentrations to achieve the actual loading capacities of the HAuNPs. Another way would be to test different pHs of different dyes. This could determine if the pH plays a role in loading. Another approach for this study would be to get the PVP synthesis of the HAuNPs to work since this study failed to make AgNPs from PVP. To take the study a step further, the HAuNPs could be made using both PVP and $NaBH_4$. Finally, a release study should be done on each dye and concentration of particles used. This release study will determine the stability, but also allow for a successful release of dye from the particles.

Conclusion:

This study investigates a potential drug delivery system using hollow gold nanoparticles. The synthesis of hollow gold nanoparticles (HAuNPs) using a galvanic replacement reaction was successful, with the HAuNPs exhibiting a plasmon peak at 980 nm, which makes these HAuNPs suitable for a potential drug delivery system and possible targeted therapy treatment for cancer. The study also examined the loading efficacy of model dyes (Methyl Orange, Acid Orange 5, and Chrysione Resorcinol) into the HAuNPs. The data showed that the HAuNPs preferred Acid Orange 5 when binding, but loaded higher concentrations of Methyl Orange. This was shown with Acid Orange having a higher K value of 0.04 and Methyl Orange having a higher coverage value of 1.03 (not washed) and 0.5 (washed). This suggests that the drug used in combination with HAuNPs must either bind well with the surface sites of the HAuNPs or have a higher dosage in order to cover all the surface sites. Further research is needed to determine the actual loading capacities of these HAuNPs, but data suggests that HAuNPs have the potential for strong binding/loading interactions with dyes.

Resources.

1. Zugazagoitia, Jon, MD, PhD, Guedes, C., MD, Ponce, S., MD, Ferrer, I., PhD, Molina-Pinelo, S., PhD, and Paz-Ares, Luis, MD, PhD. (2016) Current challenges in cancer treatment. *Clinical therapeutics. 38*, 1551-1566.

2. Lee, Y. T., Tan, Y. J., and Oon, C. E. (2018) Molecular targeted therapy: Treating cancer with specificity. *European journal of pharmacology. 834*, 188-196.

3. Sanna, V., Pala, N., and Sechi, M. (2014) Targeted therapy using nanotechnology: Focus on cancer. *International Journal of Nanomedicine. 9*, 467-483.

4. Tariq, H., and Bokhari, S. A. I. (2020) Surface-functionalized hybrid nanoparticles for targeted treatment of cancer. *IET nanobiotechnology. 14*, 537-547.

5. Debela, D. T., Muzazu, S. G. Y., Heraro, K. D., Ndalama, M. T., Mesele, B. W., Haile, D. C., Kitui, S. K., and Manyazewal, T. (2021) *New approaches and procedures for cancer treatment: Current perspectives.* SAGE Publications Ltd, .

6. Begines, B., Ortiz, T., Pérez-Aranda, M., Martínez, G., Merinero, M., Argüelles-Arias, F., and Alcudia, A. (2020) Polymeric nanoparticles for drug delivery: Recent developments and future prospects. *Nanomaterials (Basel, Switzerland). 10*, 1403.

7. Park, J., Choi, H. E., Kudaibergen, D., Kim, J., and Kim, K. S. (2021) Recent advances in hollow gold nanostructures for biomedical applications. *Frontiers in chemistry. 9*, 699284.

8. Alkilany, A. M., and Murphy, C. J. (2010) Toxicity and cellular uptake of gold nanoparticles: What we have learned so far? *J Nanopart Res. 12*, 2313-2333.

9. Kumar, A., Das, N., Satija, N. K., Mandrah, K., Roy, S. K., and Rayavarapu, R. G. (2019) *A novel approach towards synthesis and characterization of non-cytotoxic gold nanoparticles using taurine as capping agent.* MDPI AG, .

10. Sidhu, A. K., Verma, N., and Kaushal, P. (2022) Role of biogenic capping agents in the synthesis of metallic nanoparticles and evaluation of their therapeutic potential. *Frontiers in nanotechnology. 3*.

11. Khatoon, U. T., Velidandi, A., and Nageswara Rao, G. V. S. (2023) Sodium borohydride mediated synthesis of nano-sized silver particles: Their characterization, anti-microbial and cytotoxicity studies. *Materials chemistry and physics. 294*, 126997.

12. Valencia, F. J., Ramírez, M., Varas, A., Rogan, J., and Kiwi, M. (2020) *Thermal stability of hollow porous gold nanoparticles: A molecular dynamics study.* American Chemical Society (ACS), .

13. Schwartzberg, A. M., Olson, T. Y., Talley, C. E., and Zhang, J. Z. (2006) Synthesis, characterization, and tunable optical properties of hollow gold nanospheres. *The journal of physical chemistry. B. 110*, 19935-19944.

14. SUTTON, D., NASONGKLA, N., BLANCO, E., and JINMING GAO. (2007) Functionalized micellar systems for cancer targeted drug delivery. *Pharmaceutical research. 24*, 1029-1046.

15. Xiong, C., Lu, W., Zhou, M., Wen, X., and Li, C. (2018) Cisplatin-loaded hollow gold nanoparticles for laser-triggered release. *Cancer Nano. 9*, 6-13.

16. You, J., Zhang, G., and Li, C. (2010) Exceptionally high payload of doxorubicin in hollow gold nanospheres for near-infrared light-triggered drug release. *ACS nano. 4*, 1033-1041.

17. Anselmo, A. C., and Mitragotri, S. (2019) Nanoparticles in the clinic: An update. *Bioengineering & Translational Medicine. 4*, e10143-n/a.

18. Yasun, E., Gandhi, S., Choudhury, S., Mohammadinejad, R., Benyettou, F., Gozubenli, N., and Arami, H. (2020) Hollow micro and nanostructures for therapeutic and imaging applications. *Journal of drug delivery science and technology. 60*, 102094.

19. Patra, J. K., Das, G., Fraceto, L. F., Campos, E. V. R., Rodriguez-Torres, M. D. P., Acosta-Torres, L. S., Diaz-Torres, L. A., Grillo, R., Swamy, M. K., Sharma, S., Habtemariam, S., and Shin, H. (2018) *Nano based drug delivery systems: Recent developments and future prospects.* Springer Science and Business Media LLC, .

20. Yao, Y., Zhou, Y., Liu, L., Xu, Y., Chen, Q., Wang, Y., Wu, S., Deng, Y., Zhang, J., and Shao, A. (2020) Nanoparticle-based drug delivery in cancer therapy and its role in overcoming drug resistance. *Frontiers in molecular biosciences. 7*, 193.

21. Donahue, N. D., Acar, H., and Wilhelm, S. (2019) Concepts of nanoparticle cellular uptake, intracellular trafficking, and kinetics in nanomedicine. *Advanced drug delivery reviews. 143*, 68-96.

22. A. Rydströ, M.S. Deshayes, K. Konate, L. Crombez, K. Padari, Direct translocation as major cellular uptake for cady self-assembling peptide-based nanoparticles, PLoS ONE 6 (2011) 25924, https://doi.org/10.1371/journal.pone. 0025924.

23. P. Guterstam, F. Madani, H. Hirose, T. Takeuchi, S. Futaki, S. El, A. Gräslund, Ü. Langel, Elucidating cell-penetrating peptide mechanisms of action for membrane interaction, cellular uptake, and translocation utilizing the hydrophobic counteranion pyrenebutyrate, BBA Biomembr. 1788 (2009) 2509–2517, https://doi.org/ 10.1016/j.bbamem.2009.09.014.

24. W.B. Kauffman, T. Fuselier, J. He, W.C. Wimley, Mechanism matters: a taxonomy of cell penetrating peptides, Trends Biochem. Sci. 40 (2015) 749–764, https://doi.org/ 10.1016/j.tibs.2015.10.004.

25. Harish V, Ansari MM, Tewari D, Gaur M, Yadav AB, García-Betancourt ML, Abdel-Haleem FM, Bechelany M, Barhoum A. Nanoparticle and Nanostructure Synthesis and Controlled Growth Methods. Nanomaterials (Basel). 2022 Sep 16;12(18):3226. doi: 10.3390/nano12183226. PMID: 36145012; PMCID: PMC9503496.

26. Villanueva-Flores, F., Castro-Lugo, A., Ramírez, O. T., and Palomares, L. A. (2020) *Understanding cellular interactions with nanomaterials: Towards a rational design of medical nanodevices*. IOP Publishing, .

27. Pan Y, Neuss S, Leifert A, Fischler M, Wen F, Simon U, Schmid G, Brandau W, Jahnen-Dechent W. Size-dependent cytotoxicity of gold nanoparticles. *Small.* 2007;3:1941–9. doi: 10.1002/smll.200700378.

28. Tsoli M, Kuhn H, Brandau W, Esche H, Schmid G. Cellular Uptake and Toxicity of Au55 Clusters. *Small.* 2005;1:841–4. doi: 10.1002/smll.200500104.

29. Senut M-C, Zhang Y, Liu F, Sen A, Ruden D M, Mao G. Size-dependent toxicity of gold nanoparticles on human embryonic stem cells and their neural derivatives. *Small.* 2016;12:631–46. doi: 10.1002/smll.201502346.

30. Chithrani B D, Ghazani A A, Chan W C W. Determining the size and shape dependence of gold nanoparticle uptake into mammalian cells. *Nano Lett.* 2006;6:662–8. doi: 10.1021/nl052396o

31. Alhalili Z. Metal Oxides Nanoparticles: General Structural Description, Chemical, Physical, and Biological Synthesis Methods, Role in Pesticides and Heavy Metal Removal through Wastewater Treatment. Molecules. 2023 Mar 30;28(7):3086. doi: 10.3390/molecules28073086.

32. Zielińska A, Carreiró F, Oliveira AM, Neves A, Pires B, Venkatesh DN, Durazzo A, Lucarini M, Eder P, Silva AM, Santini A, Souto EB. Polymeric Nanoparticles: Production, Characterization, Toxicology and Ecotoxicology. Molecules. 2020 Aug 15;25(16):3731. doi: 10.3390/molecules25163731.

33. Sun, L., Lv, H., Feng, J., Guselnikova, O., Wang, Y., Yamauchi, Y., and Liu, B. (2022) *Noble‐Metal‐Based hollow mesoporous nanoparticles: Synthesis strategies and applications.* Wiley, .

34. Talarska, P., Boruczkowski, M., and Żurawski, J. (2021) Current knowledge of silver and gold nanoparticles in laboratory Research—Application, toxicity, cellular uptake. *Nanomaterials (Basel, Switzerland). 11*, 2454.

35. Ren, Q., Bai, L., Zhang, X., Ma, Z., Liu, B., Zhao, Y., and Cao, Y. (2015) Preparation, modification, and application of hollow gold nanospheres. *Journal of Nanomaterials. 2015*, 1-7.

36. Wang, Y., Rhéaume, É, Lesage, F., and Kakkar, A. (2018) *Synthetic methodologies to gold nanoshells: An overview.* MDPI AG, .

37. Sun, Y., and Xia, Y. (2003) Alloying and dealloying processes involved in the preparation of metal nanoshells through a galvanic replacement reaction. *Nano letters. 3*, 1569-1572.

38. Ashenhurst, James. "Sodium Borohydride (NABH4) Reduction of Aldehydes and Ketones." *Master Organic Chemistry*, 22 May 2023, www.masterorganicchemistry.com/2011/08/12/reagent-friday-sodium-borohydride-nabh4/.

39. Trotsiuk, L., Antanovich, A., Lizunova, A., and Kulakovich, O. (2020) Direct synthesis of amphiphilic polyvinylpyrrolidone-capped gold nanoparticles in chloroform. *Colloid and interface science communications. 37*, 100289.

40. Javed, R., Sajjad, A., Naz, S., Sajjad, H., and Ao, Q. (2022) Significance of capping agents of colloidal nanoparticles from the perspective of drug and gene delivery, bioimaging, and biosensing: An insight. *International journal of molecular sciences. 23*, 10521.

41. Sun, Y.; Xia, Y. Shape-Controlled Synthesis of Gold and Silver Nanoparticles. Science (80-.). 2002, 298, 2176–2179.

42. Soilis, Z. M. (2020) *Alizarin red S loaded poly (vinyl pyrrolidone) capped hollow gold nanoparticles: A model drug delivery device.*

43. Garg E, Zubair M. Mass Spectrometer. [Updated 2023 Jan 21]. In: StatPearls [Internet]. Treasure Island (FL): StatPearls Publishing; 2024 Jan-.

44.Garza AZ, Park SB, Kocz R. Drug Elimination. [Updated 2023 Jul 4]. In: StatPearls [Internet]. Treasure Island (FL): StatPearls Publishing; 2024 Jan-.

45. De Haan, M. P., Balakrishnan, N., Kuzmyn, A. R., Li, G., Willemen, H. M., Seide, G., Derksen, G. C. H., Albada, B., and Zuilhof, H. (2021) *Alizarin grafting onto ultrasmall ZnO nanoparticles: Mode of binding, stability, and colorant studies.* American Chemical Society (ACS), .

46. Ma, R., Tang, S., Tan, H., Lin, W., Wang, Y., Wei, J., Zhao, L., and Tang, T. (2014) Preparation, characterization, and in vitro osteoblast functions of a nano-hydroxyapatite/polyetheretherketone biocomposite as orthopedic implant material. *International Journal of Nanomedicine. 9*, 3949-3961.

47. National Center for Biotechnology Information. "PubChem Compound Summary for CID 135436535, Chrysoine" *PubChem*, https://pubchem.ncbi.nlm.nih.gov/compound/Chrysoine. Accessed 13 November, 2023.

48. Zhukova, V., Osipova, N., Semyonkin, A., Malinovskaya, J., Melnikov, P., Valikhov, M., Porozov, Y., Solovev, Y., Kuliaev, P., Zhang, E., Sabel, B. A., Chekhonin, V., Abakumov, M., Majouga, A., Kreuter, J., Henrich-Noack, P., Gelperina, S., and Maksimenko, O. (2021) Fluorescently labeled PLGA nanoparticles for visualization in vitro and in vivo: The importance of dye properties. *Pharmaceutics. 13*, 1145.

49. Dizaj, S. M., Vazifehasl, Z., Salatin, S., Adibkia, K., and Javadzadeh, Y. (2015) Nanosizing of drugs: Effect on dissolution rate. *Research in Pharmaceutical Sciences. 10*, 95-108.

50. National Center for Biotechnology Information. "PubChem Compound Summary for CID 23673835, Methyl orange" *PubChem*, https://pubchem.ncbi.nlm.nih.gov/compound/Methyl-orange. Accessed 13 November, 2023.

51. National Center for Biotechnology Information. "PubChem Compound Summary for CID 23668839, Tropaeolin OO" *PubChem*, https://pubchem.ncbi.nlm.nih.gov/compound/Tropaeolin-OO. Accessed 13 November, 2023.

52. Rasmussen, M. K., Pedersen, J. N., and Marie, R. (2020) *Size and surface charge characterization of nanoparticles with a salt gradient.* Springer Science and Business Media LLC, .

53. Ivanov MR, Bednar HR, Haes AJ. Investigations of the mechanism of gold nanoparticle stability and surface functionalization in capillary electrophoresis. ACS Nano. 2009 Feb 24;3(2):386-94.

54. Gallina, C., Capelôa, T., Saviozzi, S., Accomasso, L., Catalano, F., Tullio, F., Martra, G., Penna, C., Pagliaro, P., Turinetto, V., and Giachino, C. (2015) *Human mesenchymal stem cells labelled with dye-loaded amorphous silica nanoparticles: Long-term biosafety, stemness preservation and traceability in the beating heart.* Springer Science and Business Media LLC, .

55. Zoubari, G., Staufenbiel, S., Volz, P., Alexiev, U., and Bodmeier, R. (2017) Effect of drug solubility and lipid carrier on drug release from lipid nanoparticles for dermal delivery. *European journal of pharmaceutics and biopharmaceutics. 110*, 39-46.

56. Stewart, A. M., and Grass, M. E. (2020) Practical approach to modeling the impact of amorphous drug nanoparticles on the oral absorption of poorly soluble drugs. *Molecular pharmaceutics. 17*, 180-189.

57. Dung, N. T., Linh, N. T. N., Chi, D. L., Hoa, N. T. H., Hung, N. P., Ha, N. T., Nam, P. H., Phuc, N. X., Tam, L. T., and Lu, L. T. (2021) Optical properties and stability of small hollow gold nanoparticles. *RSC advances. 11*, 13458-13465.

58. Jalani G, Tam V, Vetrone F, Cerruti M. Seeing, Targeting and Delivering with Upconverting Nanoparticles. J Am Chem Soc. 2018 Sep 5;140(35):10923-10931. doi: 10.1021/jacs.8b03977. Epub 2018 Aug 16.

59. Shikha, S., Dureja, S., Sapra, R., Babu, J., Haridas, V., and Pattanayek, S. K. (2021) *Interaction of borohydride stabilized silver nanoparticles with sulfur-containing organophosphates.* Royal Society of Chemistry (RSC).

60. Mavani, K., and Shah, M. *Synthesis of silver nanoparticles by using sodium borohydride as a reducing agent.*

61. Swenson, H., and Stadie, N. P. (2019) *Langmuir's theory of adsorption: A centennial review.* American Chemical Society (ACS), .

62. Shen, L.; Wang, Z.; Fang, S.; Liu, Y. Biosorption Isotherms and Thermodynamics. In Fundamentals and Applications of Biosorption Isotherms, Kinetics and Thermodynamics; Liu, Y., Wang, J., Eds.; Nova Science Publishers, Inc.: New York, 2009; pp 7–9.

63. Langmuir, I. The Adsorption of Gases on Plane Surfaces of Glass, Mica and Platinum. J. Am. Chem. Soc. 1918, 40 (9), 1361–1403.

64. Azizian, S.; Eris, S.; Wilson, L. D. Re-Evaluation of the Century-Old Langmuir Isotherm for Modeling Adsorption Phenomena in Solution. Chem. Phys. 2018, 513 (May), 99–104.

65. Cavuslar, O., Nakay, E., Kazakoglu, U., Abkenar, S. K., Ow-Yang, C. W., and Acar, H. Y. (2020) *Synthesis of stable gold nanoparticles using linear polyethyleneimines and catalysis of both anionic and cationic azo dye degradation.* Royal Society of Chemistry (RSC), .

66. Ahsan, H., Shahid, M., Imran, M., Mahmood, F., Siddique, M. H., Ali, H. M., Niazi, M. B. K., Hussain, S., Shahbaz, M., Ayyub, M., and Shahzad, T. (2022) *Photocatalysis and adsorption kinetics of azo dyes by nanoparticles of nickel oxide and copper oxide and their nanocomposite in an aqueous medium.* PeerJ, .

67. Bokare, A. D., Chikate, R. C., Rode, C. V., and Paknikar, K. M. (2007) *Effect of surface chemistry of Fe−Ni nanoparticles on mechanistic pathways of azo dye degradation.* American Chemical Society (ACS), .

68. "Derivation of the Langmuir Isotherm." *Derivation of the Langmuir Isotherm*, pages.jh.edu/chem/fairbr/teach/BET/lang.html#:~:text=Kinetic%20Derivation&text=where%20b%3Dka%2Fk,and%20gas%20phase%20species%20involved. Accessed 10 Apr. 2024.

69. Chen, T., Li, M., and Liu, J. (2018) *Π–π stacking interaction: A nondestructive and facile means in material engineering for bioapplications.* American Chemical Society (ACS), .